ELSEVIER

Biochemical Pharmacology 63 (2002) 81–88

Biochemical Pharmacology

Fluorescein uptake by a monocarboxylic acid transporter in human intestinal Caco-2 cells

Kenji Kuwayama[a], Seiji Miyauchi[a,*], Ryoko Tateoka[a], Hiroshi Abe[b], Naoki Kamo[a]

[a]*Laboratory of Biophysical Chemistry, Graduate School of Pharmaceutical Sciences, Hokkaido University, Sapporo 060-0812, Japan*
[b]*Laboratory of Medicinal Chemistry, Graduate School of Pharmaceutical Sciences, Hokkaido University, Sapporo 060-0812, Japan*

Received 11 July 2000; accepted 22 May 2001

Abstract

The fluorescein transport characteristics of the human intestinal epithelial Caco-2 cell line were examined in monolayer cultures. The initial uptake rate was concentration-dependent and saturable; the Michealis constant and the maximum velocity were 0.40 mM and 1.32 nmol/min/mg protein, respectively. A protonophore, carbonyl cyanide *m*-chlorophenyl-hydrazone, reduced uptake significantly. The replacement of extracellular sodium ions by lithium ions did not alter the initial uptake rate. These facts imply that the transport is driven by a proton gradient. The initial uptake rate was strongly dependent upon extracellular pH, and the uptake was optimal at approximately pH 5.5. Based on the protolytic constants, the main species of fluorescein in the pH range of 5.5 to 6.0 was calculated to be a monoanion, suggesting that fluorescein was taken up by Caco-2 cells as a monocarboxylate. The following findings support this conclusion: the uptake was inhibited significantly by monocarboxylate compounds such as salicylate and pravastatin, but not by di- or tricarboxylic acids or by acidic amino acids. Furthermore, salicylate-preloaded cells showed remarkably enhanced uptake of fluorescein, indicating that monocarboxylates and fluorescein share a common transport carrier. The transporter has a wide spectrum of substrate recognition and seems likely to be different from MCT1.

Keywords: Fluorescein; Monocarboxylic acid transporter; Caco-2 cells; Salicylate; Intestinal absorption

1. Introduction

Fluorescein is an extensively used fluorescent dye, because of its large quantum yield and high photostability [1]. The flexibility of the many label derivatives makes this dye useful: fluorescein derivatives such as fluorescein isothiocyanate and fluorescein succinimidyl ester can be attached to macromolecules, peptides [2], or oligonucleotides covalently [3] and are commercially available. The molecules labeled by fluorescein possess superior stability and comparable fluorescence, and are utilized to detect macromolecules in electrophoresis gels [4], on nitrocellulose membranes [5], and in cells [6].

Conjugates of fluorescein have been used to determine the behavior of target compounds; for example, fluorescein conjugates to methotrexate and bile acid were used for characterization of the folate transporter [7], multidrug resistance associated protein [8], and bile salt transporter [9]. These conjugates are believed to be recognized by transporters as true ligands, since fluorescein itself might be transported across the cell membrane by passive diffusion rather than by membrane transporters. However, it has been reported recently that fluorescein is secreted into urine by a classical and a specific organic anion transporter [10–12]. This implies that caution must be exercised when a fluorescein conjugate is used as a substrate to investigate transporter kinetics.

These circumstances led us to undertake a transport study of fluorescein itself. As far as we know, such work on fluorescein has not been carried out except on urinary excretion. In the present study, we determined the transport mechanism of fluorescein in intestinal absorption using the Caco-2 cell line. Caco-2 cells spontaneously differentiate in culture into polarized cell monolayers with microvilli, which mimic the properties of small intestinal epithelial cells [13,14]. The Caco-2 cell line is a useful model to study absorption in the small intestine, since these cells retain a

* Corresponding author. Tel: +81-11-706-3936; fax: +81-11-706-4984.
E-mail address: miya@pharm.hokudai.ac.jp (S. Miyauchi).

Abbreviations: CCCP, carbonyl cyanide *m*-chlorophenylhydrazone; CHC, α-cyano-4-hydroxycinnamic acid; DIDS, 4,4′-diisothiocyanostilbene-2,2′-disulfonic acid; MES, 2-(*N*-morpholino)ethanesulfonic acid; and Tris, Tris(hydroxymethyl)-aminomethane.

0006-2952/02/$ – see front matter
PII: S0006-2952(01)00853-X

number of solute transport systems including those for amino acids [15], sugars [16], phosphate [17], bile acids [18], and dipeptide [19]. We showed that the uptake of fluorescein by Caco-2 cells occurs via a proton-gradient dependent carrier that also transports other monocarboxylate compounds, such as salicylate.

2. Materials and methods

2.1. Materials

CCCP, CHC, DIDS, and firefly lantern extract were purchased from the Sigma Chemical Co. Pravastatin was extracted from mevalotin (Sankyo Co.) and purified. Dullbecco's modified Eagle's medium (DMEM), MEM non-essential amino acids, and fetal bovine serum (FBS) were purchased from GIBCO-BRL Life Technologies. Fluorescein was purchased from Molecular Probes, Inc. All other chemicals used were of the highest purity available.

2.2. Cell culture

Caco-2 cells (ATCC HTB-37) at passage 28 were purchased from the American Type Culture Collection. They were passaged in 75 cm^2 culture flasks (FALCON, Becton Dickinson) in culture medium consisting of DMEM supplemented with 1% MEM non-essential amino acids and FBS (15%), HEPES (5 mM), and $NaHCO_3$ (2 g/L) without antibiotics. The cells were maintained at 37° in an atmosphere of 5% CO_2. Cells between the 30th and 40th passage were used in this study. At approximately 80% confluence, cells were seeded using 0.02% EDTA and 0.05% trypsin at a density of 53,000 cells/cm^2 on a 60-mm plastic culture dish. The cells were fed fresh medium every 3 days, and were used for transport studies between days 14 and 16.

2.3. Uptake experiments in Caco-2 cell monolayers

The uptake of fluorescein was measured in cells grown in plastic culture dishes. The composition of the incubation medium was 140 mM NaCl, 3 mM KCl, 1 mM $CaCl_2$, 1 mM $MgCl_2$, 5 mM d-glucose, 5 mM MES (pH 6.0), or 5 mM HEPES (pH 7.4). After removal of the culture medium, each dish was washed once with 5 mL of the incubation medium (pH 7.4) prewarmed at 37° and incubated with 2 mL of the same medium for 10 min at 37°. After removal of the medium, the cells were incubated with 1.5 mL of incubation medium (pH 6.0) containing fluorescein in the absence or the presence of inhibitor for a designated period at 37°. Thereafter, the medium was aspirated off, and the dishes were rinsed twice rapidly with ice-cold incubation medium (pH 7.4). In the case of zero time, after addition of the incubation medium (pH 7.4 or 6.0) it was immediately aspirated off, and the dishes were rinsed with the ice-cold medium (pH 7.4). This washing procedure was completed in less than 20 sec. The cells were solubilized in 1 mL of 1 N NaOH and neutralized by 1 mL of 1 N HCl. The extraction solution was centrifuged at 15,000 *g* for 5 min at 4° in a table-top microfuge (Hitachi). The supernatant was diluted with 1 M Tris buffer (pH 9.8). The fluorescence intensity attributed to fluorescein derivatives was determined with a Hitachi F-4500 fluorometer (Hitachi) with emission at 525 ± 3 nm and excitation at 490 ± 3 nm. When the uptake of fluorescein was measured in the presence of CCCP or 10 μM oligomycin plus 50 mM 2-deoxyglucose, the cells were preincubated for 10 min at the same temperature with 1.5 mL of incubation medium (pH 6.0) containing 40 μM CCCP or 10 μM oligomycin plus 50 mM 2-deoxyglucose and then incubated for the designated period at 37° with 1.5 mL of incubation medium (pH 6.0) containing 40 μM CCCP or 10 μM oligomycin plus 50 mM 2-deoxyglucose. For measurement of the countertransport effect, salicylate was preloaded into cells by exposing them to incubation medium (pH 6.0) containing 20 mM salicylate for 10 min at 37°. The salicylate-containing medium was aspirated off, and the cells were washed with 2 mL of incubation medium (pH 6.0), and then immediately treated for the designated time at 37° with 1.5 mL of incubation medium (pH 6.0) containing 50 μM fluorescein. Thereafter, the cells were treated in a manner similar to that described above. In all uptake measurements, unless otherwise indicated, values were corrected for protein content. The protein content of the cell monolayers solubilized in 1.0 mL of 1 M NaOH was determined using a Bio-Rad protein assay kit (Bio-Rad Laboratories) with bovine serum albumin as the standard.

2.4. Measurement of intracellular ATP level

Cells grown on plastic culture dishes were incubated in the absence or presence of 10 μM oligomycin plus 50 mM 2-deoxyglucose (pH 7.4) during a 10-min period. After a preincubation period, cells were incubated for 10 min at 37° in the absence or presence of 10 μM oligomycin plus 50 mM 2-deoxyglucose (pH 6.0). Thereafter, the medium was aspirated off, and the dishes were rapidly rinsed twice with an ice-cold incubation medium (pH 7.4). The cells were treated immediately with 500 μL of 5% perchloric acid. After neutralization with 1 M KOH and centrifugation for 1 min at 15,000 *g* and 4° in the table-top microfuge, the supernatant was used for the determination of ATP with a J4–7441 Chem-Glow Photometer (American Instrument) utilizing firefly lantern extract [20].

2.5. Kinetic analysis of fluorescein uptake

The fluorescein uptake data were fitted to a Michaelis–Menten type equation with a saturable component and a nonsaturable component by the iterative nonlinear least-squares method in Origin (MicroCal):

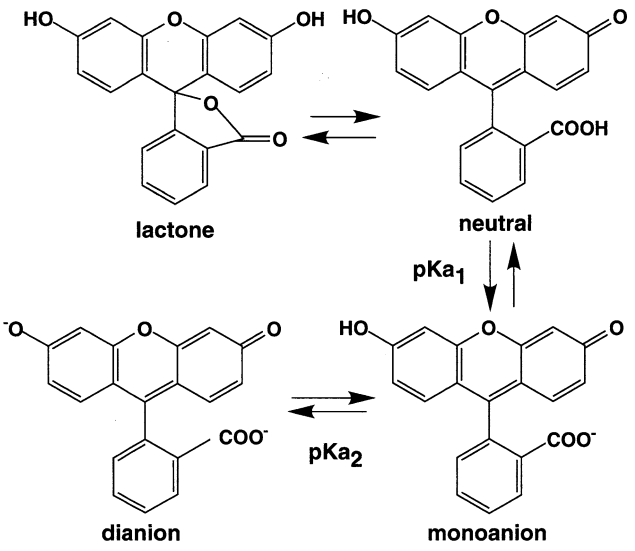

Fig. 1. Ionization equilibria of fluorescein. A systematic study by Zanker and Peter [21] demonstrated that there are three molecular species: the neutral, monoanion, and dianion forms of fluorescein.

$$V_0 = V_{max}[S]/(K_m+[S])+K_d[S] \quad (1)$$

where V_0 represents the initial uptake rate of fluorescein; V_{max}, the maximum uptake velocity; [S], the initial concentration of Gly-Sar; K_m, the Michaelis constant; and K_d, the coefficient of passive diffusion.

2.6. Absorption spectra of fluorescein

The absorption spectra of fluorescein at various pH levels were determined utilizing a V-560 spectrophotometer (Nihonbunko, Ltd. Co.). Zanker and Peter [21] were the first to perform systematic studies of ion species. Lindquist [22] partially identified the individual absorption spectra of the neutral (N), monoanion (MA), and dianion (DA) forms of fluorescein (Fig. 1). His study clearly showed that the main molecular species at pH 10.0 and 3.0 are dianion and neutral species of fluorescein, respectively. According to the results, the absorption spectra at any pH were expressed as the following equation:

$$\begin{aligned}\mathrm{Abs}(\lambda)_{pH} &= 1/(1+10^{pH\text{-}pK_{a1}}+10^{2pH\text{-}(pK_{a1}+pK_{a2})})\\ &\quad \mathrm{Abs}(\lambda)_{3.0}+ 10^{pH\text{-}pK_{a1}}/(1+10^{pH\text{-}pK_{a1}}\\ &+ 10^{2pH\text{-}(pK_{a1}+pK_{a2})})\mathrm{Abs}(\lambda)_{MA}\\ &+ 10^{2pH\text{-}(pK_{a1}+pK_{a2})}/(1+10^{pH\text{-}pK_{a1}}\\ &+ 10^{2pH\text{-}(pK_{a1}+pK_{a2})})\mathrm{Abs}(\lambda)_{10.0} \quad (2)\end{aligned}$$

where $\mathrm{Abs}(\lambda)_{pH}$, $\mathrm{Abs}(\lambda)_{3.0}$ and $\mathrm{Abs}(\lambda)_{10.0}$, and $\mathrm{Abs}(\lambda)_{MA}$ stand for the absorption spectra at any pH, pH = 3.0 and 10.0, and absorption spectra of the MA form of fluorescein, respectively, and pK_{a1} and pK_{a2} stand for the protolytic constants of carboxylic and phenol functional groups within fluorescein, respectively. The absorption spectra were fitted simultaneously to Eq. (2) by the iterative nonlinear least-squares method in Origin, and the values for $\mathrm{Abs}(\lambda)_{MA}$, pK_{a1}, and pK_{a2} were estimated. The molar ratios of fluorescein species at any pH were calculated based on the following equations:

$$R_N = 1/(1 + 10^{pH\text{-}pK_{a1}}+10^{2pH\text{-}(pK_{a1}+pK_{a2})}) \quad (3)$$

$$R_{MA} = 10^{pH\text{-}pK_{a1}}/(1+10^{pH\text{-}pK_{a1}}+10^{2pH\text{-}(pK_{a1}+pK_{a2})})$$

$$R_{DA} = 10^{2pH\text{-}(pK_{a1}+pK_{a2})}/(1+10^{pH\text{-}pK_{a1}} \quad (4)$$

$$+ 10^{2pH\text{-}(pL_{a1}+pK_{a2}} \quad (5)$$

where R_N, R_{MA}, and R_{DA} represent the molar ratios of neutral, monoanion, and dianion species for fluorescein, respectively.

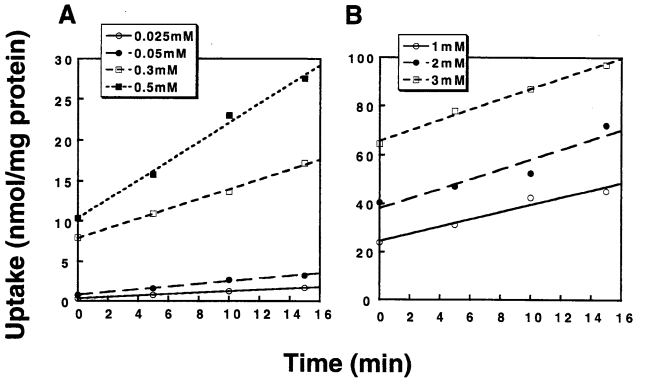

Fig. 2. Time courses of fluorescein uptake at various concentrations by Caco-2 cells. Panels A and B show the typical data of fluorescein uptake at low and high concentrations, respectively. The uptake of fluorescein was measured in incubation medium (pH 6.0). Three to four experiments were performed at various concentrations.

3. Results and discussion

3.1. Accumulation of fluorescein by Caco-2 cells

We measured the accumulation of fluorescein by Caco-2 cells. Figure 2 shows the time course for the uptake of various concentrations of fluorescein (25 μM–3 mM) by the cells. The uptake was linear with time, up to 15 min, for each concentration. The uptake rates were calculated from the slope of the lines, using linear regression analysis. The value at zero time increased linearly when the fluorescein concentration increased (Fig. 3). This value was almost the same as that at 4° and remained unchanged irrespective of various inhibitors. Thus, this value was considered to mean the rapid adsorption to the cellular surface.

The relationship between the initial uptake and concentration of fluorescein is depicted in Fig. 4. It indicates that the uptake process is comprised of a saturable process at low concentration and a nonsaturable process at high con-

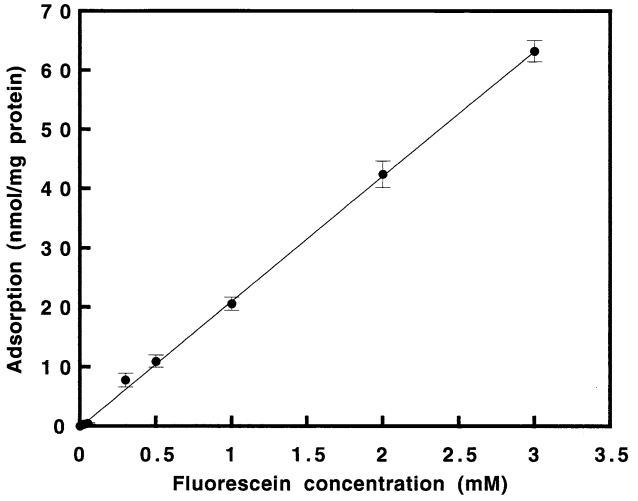

Fig. 3. Adsorption of fluorescein to the cell surface. The adsorption of fluorescein to the cell surface was estimated from the time-zero value of the time-course study. Each point is the mean ± SEM of three to four experiments.

centration. The inset in Fig. 4 shows an Eadie-Hofstee plot in which the line bends toward the horizontal axis at large velocity, revealing the existence of two processes. The kinetic parameters were calculated by fitting data to Eq. (1), and we estimated that K_m, V_{max}, and K_d were 0.40 ± 0.05 mM (± SD), 1.32 ± 0.10 nmol/min/mg protein (± SD), and 0.41 ± 0.03 μL/min/mg protein (± SD), respectively. The uptake rate at 4° was much lower than that at 37°; the uptake rate at 50 μM, 4° was 0.022 ± 0.001 nmol/min/mg protein.

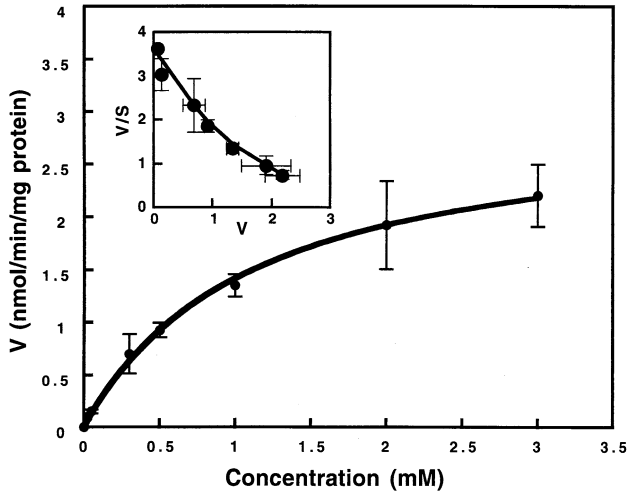

Fig. 4. Concentration-dependence of fluorescein uptake by Caco-2 cells. Initial uptake rates were determined by linear regression analysis of the linear portion of the fluorescein uptake plot. The inset shows an Eadie-Hofstee plot of fluorescein uptake. Both saturable and nonsaturable processes exist. Each point is the mean ± SEM of three to four experiments.

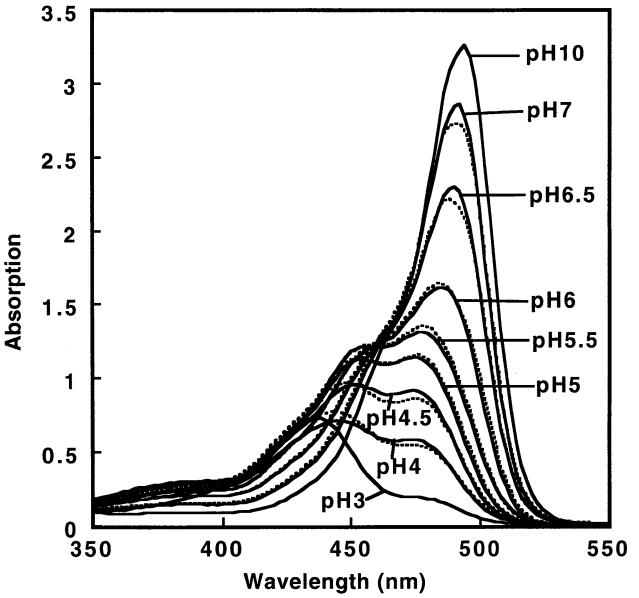

Fig. 5. Absorption spectra of fluorescein at various pH levels. The absorption spectra were simultaneously fitted to Eq. (2) by an iterative nonlinear least-squares method, and the values for pK_{a1} and pK_{a2} were estimated to be 4.36 and 6.38, respectively.

3.2. What is the ionic species of fluorescein to be transported?

As illustrated in Fig. 1, fluorescein exhibits multiple pH-dependent ionic equilibria among dianion, monoanion, and neutral species [22]. Above pH 9, protons of both the phenolic and carboxylic acid groups dissociate completely to form a dianion. Acidification of the dianion first leads to the protonation of the phenol group and yields a monoanion, followed by the protonation of the carboxyl group to yield a neutral form [22]. To determine the pK_a values, we measured the absorption spectra in the pH range of 3–10; results are shown in Fig. 5 where acidification induced the blue-shift of absorption maxima with decreased absorptivity. Simultaneous fitting of these spectra to Eq. (2) successfully determined that $pK_{a1} = 4.36$ and $pK_{a2} = 6.38$. These values are consistent with those reported by others [23].

The ionic species of fluorescein at various pH levels were calculated using Eqs. (3–5) and are depicted in Fig. 6. The pH-profile of the initial uptake rate by Caco-2 cells is overlaid in the figure. The concentration of the fluorescein used was 50 μM, where the amounts transported by the saturable component were about 85% of the total uptake at pH 6.0 based on Eq. (1). As the pH increased, the fraction of the neutral form decreased, which decreased the rate of the non-saturable component (the passive transport). The uptake rates shown in this figure, therefore, indicate the pH dependence of the amounts of fluorescein transported by a transporter. The uptake rate was optimal at approximately pH 5.5, which is the same pH where the fraction of the monoanion species is at maximum (Fig. 6). This figure also

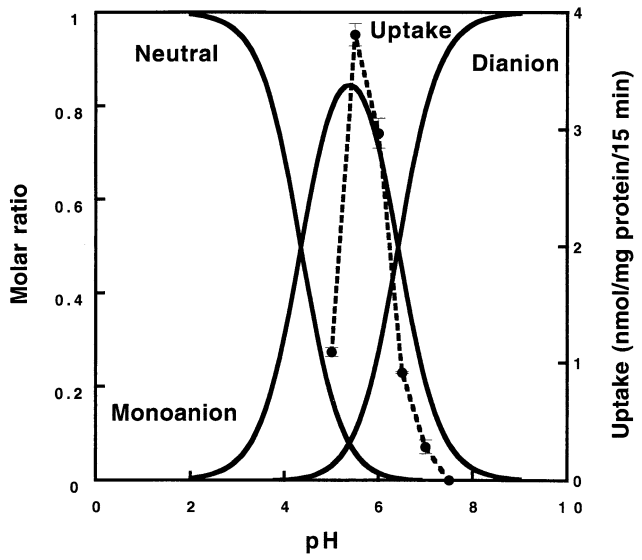

Fig. 6. Calculated molar ratios of the neutral, monoanion, and dianion forms of fluorescein. The molar ratios were predicted according to Eqs. (3–5). The uptake rate of fluorescein at 50 μM is also plotted in this figure. Good agreement exists between the molar ratio of the monoanion and the uptake of fluorescein.

reveals good agreement between the fraction of monoanion and the uptake rate at pH 8 to 5.0. These facts suggest that the monoanion species of fluorescein is transported by a transporter.

3.3. Specificity of the transporter for fluorescein

We performed an inhibition experiment using various substances. As shown in Fig. 7, the monocarboxylates salycilate, benzoate, and pravastatin were inhibitory, whereas di-or tricarboxylic acids and acidic amino acids did not reduce the uptake rate of fluorescein. The anion exchanger inhibitor DIDS, the organic anion transporter substrate *p*-aminohyppurate [24,25], and the bile acid transporter substrate taurocholic acid [26] have no effect on fluorescein uptake. These findings imply that fluorescein uptake by Caco-2 cells involves a monocarboxylate transporter. Such a monocarboxylate transporter was first documented by Tsuji, Tamai, and colleagues [27–30], who demonstrated using brush border membrane vesicles (BBMVs) and Caco-2 monolayers that the intestinal absorption of several monocarboxylates involves this transporter.

3.4. Trans-stimulation of fluorescein uptake by preloaded salicylate

To determine whether fluorescein is taken up through the monocarboxylate transporter, a trans-stimulation experiment was performed using cells preloaded with salicylate. As shown in Fig. 8, by preloading with 20 mM salicylate, the uptakes of fluorescein at 3 and 5 min were enhanced significantly. In contrast, the uptake by Caco-2 cells loaded with 20 mM citric acid remained unchanged (data not shown). These data clearly reveal that fluorescein and salicylate are transported through a common monocarboxylate transporter.

3.5. Monocarboxylate transporters in small intestine and colon

Tamai, Tsuji, and their colleagues extensively demonstrated, using BBMVs and Caco-2 cells, that monocarboxylates with bulky groups such as benzoate [29], nicotinate [27], salicylate [28], and pravastatin [30] are taken up by a common carrier that is driven by an inwardly directed H^+ gradient. On the other hand, Takagi *et al.* [31] proposed a mechanism by which salicylate is taken up via a passive diffusion process according to the pH-partition theory. They demonstrated using liposomes consisting of egg yolk phosphatidylcholine that in the presence of an inward H^+ gradient, salicylate was taken up rapidly by liposomes showing overshoot, saturation, and competitive inhibition phenomena. The present observations (a) that the substrate transported is monoanionic in nature, and (b) that it is trans-stimulated by salicylate cannot be explained by the pH-partition theory, but, rather, confirm carrier transport. Of course, we cannot dispute that salicylate or fluorescein are not also taken up by passive diffusion, because Fig. 4 shows the existence of the passive diffusion.

Various animal cells take up monocarboxylates through transporters present in these cells [32,33]. To date, nine isoforms of proton-linked monocarboxylate transporters (MCTs) have been identified in mammals, each having a different tissue distribution [32,33]. Direct demonstration of the proton-linked transport of monocarboxylate has been done for MCT1–MCT4 [34–39]. Our present system of fluorescein uptake (50 μM at pH 6.0) is also proton-linked since: replacement of extracellular Na^+ with Li^+ or addition of an anion exchanger inhibitor, DIDS at 1 mM, did not change the uptake rate [105 $\pm$ 10% (N = 5)] compared with the controls [92 $\pm$ 3 (N = 5)]; 40 μM CCCP reduced the uptake rate to 2 $\pm$ 3%; 10 μM oligomycin plus 50 mM 2-deoxyglucose changed the uptake rate slightly (93 $\pm$ 12%), although 10 μM oligomycin plus 50 mM 2-deoxyglucose remarkably reduced it to 20.8 $\pm$ 2.3% of the control (i.e. at normal intracellular ATP levels: 13 $\pm$ 1.4 nmol/mg protein) (Fig. 9).

Detailed characterizations of only two isoforms, MCT1 and MCT2, with regard to substrates and inhibitor kinetics have been achieved using a heterologous expression system. It was demonstrated recently that at least three isoforms of MCT (MCT4, MCT5, and MCT8) are present in the small intestine and colon [32,33]. MCT1 is believed to play an important role in the uptake of lactate, pyruvate, and short-chain fatty acids such as butylate and propionate from the intestinal lumen into the blood [32,40]. On the other hand, monocarboxylates with longer branched aliphatic or aro-

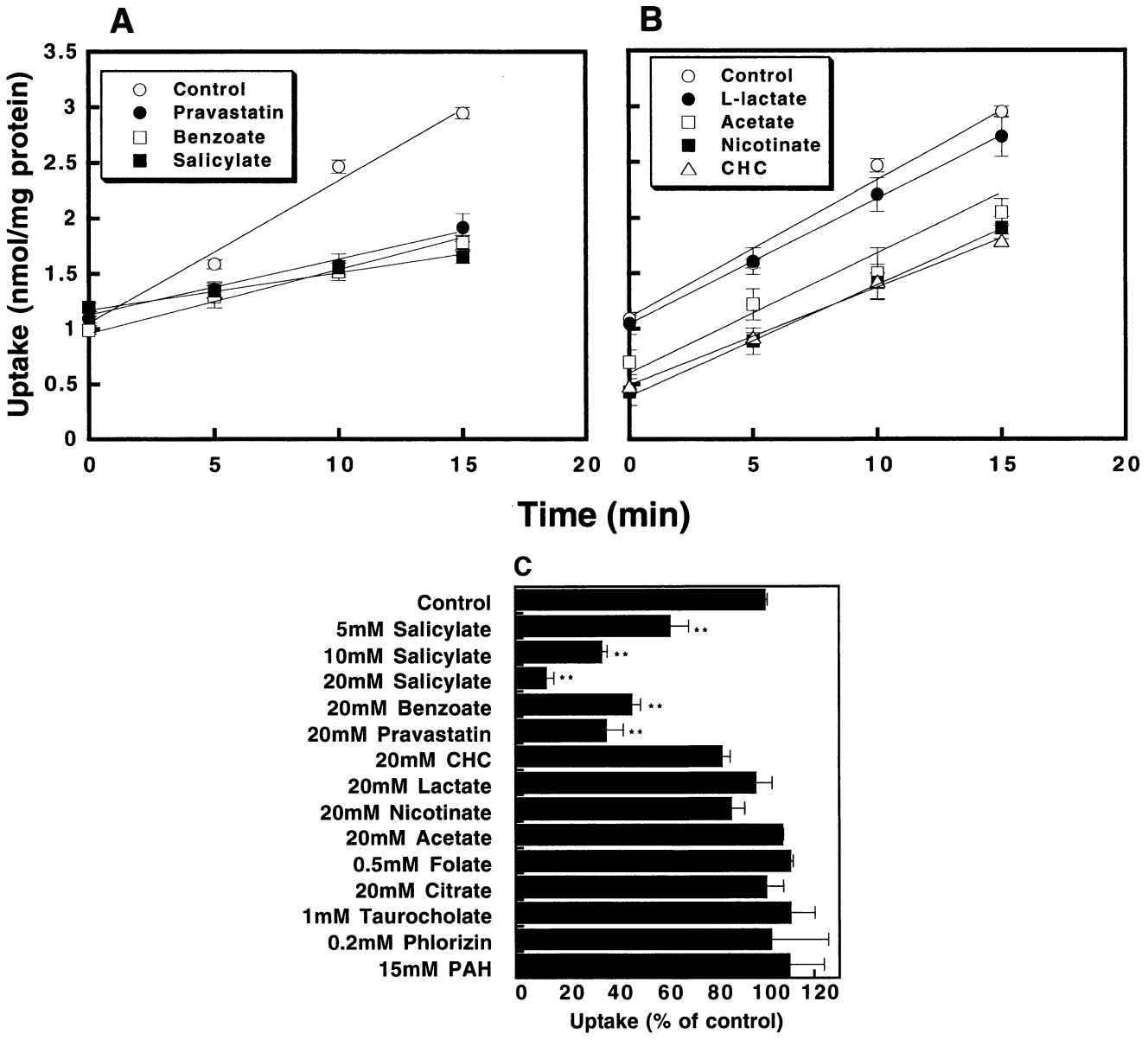

Fig. 7. Inhibitory effect of various compounds on the transport of fluorescein. The uptake rate of 50 μM fluorescein was measured in the absence or presence of various compounds. Panels (A) and (B) represent time courses of fluorescein uptake under inhibitory and non-inhibitory conditions, respectively. The concentration of monocarboxylates used was 20 mM. Initial uptake rates were determined using linear regression analysis of the linear portion of the fluorescein uptake plot (0, 5, 10, 15 min). Uptake rates were normalized for the absence of compounds. Panel (C) represents the effects of various compounds on the uptake rates of fluorescein. Each value is the mean ± SEM of four experiments. Statistical analysis was done by Student's *t*-test. Key: (**) $P < 0.01$ vs control.

matic side chains bind to MCT1, but are not transported because they are not readily released following translocation [32,41]. As shown in Fig. 7, L-lactate, a good substrate for MCT1–MCT4 [32], did not inhibit the uptake rate of fluorescein. A specific inhibitor, CHC, also had no effect on the fluorescein uptake. The fluorescein uptake rate was not altered by acetate or nicotinate, although its adsorption to the cell surface was reduced by them. Considering the fact that the present transporter can transport fluorescein and salicylate, both of which have bulky aromatic rings, but not a small monocarboxylate such as lactate and acetate (Fig. 7), we can infer that MCT1–MCT4 are not involved in fluorescein transport. Identification of the fluorescein transporter and its direct demonstration using a heterologous expression system such as *Xenopus* oocytes will have to await further investigation(s).

3.6. Concluding remarks

The transport of fluorescein by Caco-2 cells has been demonstrated to occur through a proton-linked transporter common with that for the monocarboxylic compounds sa-

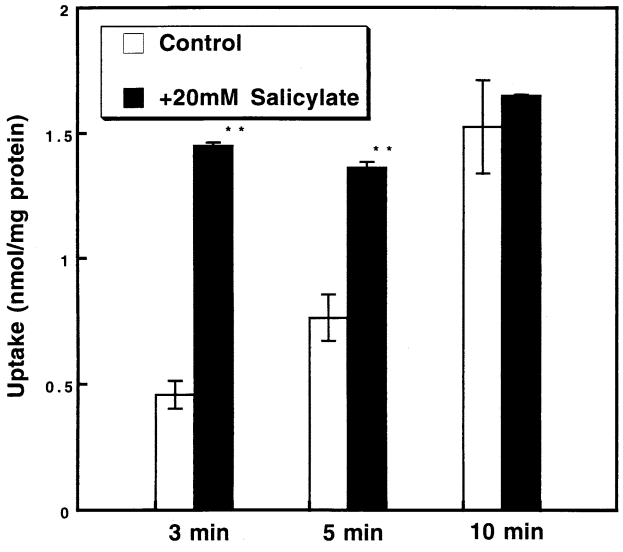

Fig. 8. Trans-stimulation of fluorescein uptake by preloaded salycilate. The cell monolayers were preloaded by incubation with 20 mM salycilate for 10 min at 37° (pH 6.0). The uptake of fluorescein was measured after incubation for a designated time at 37° (pH 6.0). Open and closed columns represent control and preloaded conditions, respectively. Each column represents the mean ± SEM of four experiments. Statistical analysis was done by Student's *t*-test. Key: (**) $P < 0.01$ vs control.

licylate, pravastatin, and nicotinate. We can infer that the transporter is not MCT1. It is worthwhile noting the diversity of substrates, but molecular interpretation requires further study. In addition, this diversity may provide good ideas for the development of new compounds useful in drug delivery. Attachment of a monocarboxylic acid group to poorly absorbed drugs might increase absorption from the small intestine.

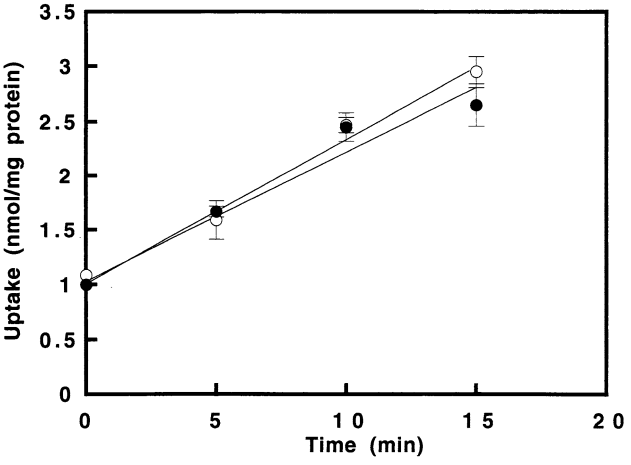

Fig. 9. Effect of intracellular ATP on the transport of fluorescein. The uptake rate of 50 μM fluorescein was measured in the absence (○) or presence of 10 μM oligomycin plus 50 mM 2-deoxyglucose (●). Initial uptake rates were determined using linear regression analysis of the linear portion of the fluorescein uptake plot (0, 5, 10, 15 min). The uptake rate was normalized for the absence of compounds. Although 10 μM oligomycin plus 50 mM 2-deoxyglucose remarkably reduced intracellular ATP to 20.8 ± 2.3% of control (intracellular ATP level under normal conditions: 13.0 ± 1.4 nmol/mg protein), the initial uptake rate of fluorescein remained unchanged. Each point represents the mean ± SEM of four experiments.

References

[1] Guilbault GG. Practical fluorescence, 2nd Edn. New York: Marcel Dekker, 1990.
[2] Vera JC, Rivas CI, Cortes PA, Carcamo JO, Delgado J. Purification, amino terminal analysis, and peptide mapping of proteins after *in situ* postelectrophoretic fluorescent labeling. Anal Biochem 1988;174: 38–45.
[3] Dirks RW, Gijlswijk RP, Tullis RH, Smit AB, Minnen J, Ploeg M, Raap AK. Simultaneous detection of different mRNA sequences coding for neuropeptide hormones by double *in situ* hybridization using FITC- and biotin-labeled oligonucleotides. J Histochem Cytochem 1990;38:467–73.
[4] Strottmann JM, Robinson JB, Stellwagen E. Advantages of preelectrophoretic conjugation of polypeptides with fluorescent dyes. Anal Biochem 1983;132:334–47.
[5] Szewczyk B, Summers DF. Fluorescent staining of proteins transferred to nitrocellulose allowing for subsequent probing with antisera. Anal Biochem 1987;164:303–6.
[6] Wells S, Johnson I. Fluorescent labels for confocal microscopy. In: Stevens JK, Mills LR, Trogadis JE, editors. Three-dimensional confocal microscopy. New York: Academic Press, 1994. p. 101–29.
[7] Fan J, Pope LE, Vitols KS, Huennekens FM. Affinity labeling of folate transport proteins with the *N*-hydroxysuccinimide ester of the γ-isomer of fluorescein-methotrexate. Biochemistry 1991;30:4573–80.
[8] Fricker G, Gutmann H, Droulle A, Drewe J, Miller DS. Epithelial transport of anthelmintic ivermectin in a novel model of isolated proximal kidney tubules. Pharm Res 1999;16:1570–5.
[9] Kitamura T, Gatmaitan Z, Arias IM. Serial quantitative image analysis and confocal microscopy of hepatic uptake, intracellular distribution and biliary secretion of a fluorescent bile acid analog in rat hepatocyte doublets. Hepatology 1990;12:1358–64.
[10] Miller DS, Letcher S, Barnes DM. Fluorescence imaging study of organic anion transport from renal proximal tubule cell to lumen. Am J Physiol 1996;271:F508–20.
[11] Masereeuw R, Russel FGM, Miller DS. Multiple pathways of organic anion secretion in renal proximal tubule revealed by confocal microscopy. Am J Physiol 1996;271:F1173–82.
[12] Masereeuw R, Moons MM, Toomey BH, Russel FGM, Miller DS. Active lucifer yellow secretion in renal proximal tubule: evidence for organic anion transport system crossover. J Pharmacol Exp Ther 1999;289:1104–11.
[13] Hidalgo IJ, Raub TJ, Borchardt RT. Characterization of the human colon carcinoma cell line (Caco-2) as a model system for intestinal epithelial permeability. Gastroenterology 1989;96:736–49.
[14] Hilgers AR, Conradi RA, Burton PS. Caco-2 cell monolayers as a model for drug transport across the intestinal mucosa. Pharm Res 1990;7:902–10.
[15] Hidalgo IJ, Borchardt RT. Transport of a large neutral amino acid (phenylalanine) in a human intestinal epithelial cell line, Caco-2. Biochim Biophys Acta 1990;1028:25–30.
[16] Blais A, Bissonnette P, Berteloot A. Common characteristics for Na^+-dependent sugar transport in Caco-2 cells and human fetal colon. J Membr Biol 1987;99:113–25.
[17] Mohrmann I, Mohrmann M, Biber J, Murer H. Sodium-dependent transport of P_i by an established intestinal epithelial cell line (Caco-2). Am J Physiol 1986;250:G323–30.
[18] Hidalgo IJ, Borchardt RT. Transport of bile acids in a human intestinal epithelial cell line, Caco-2. Biochim Biophys Acta 1990;1035: 97–103.

[19] Dantzig AH, Bergin L. Uptake of the cephalosporin, cephalexin, by a dipeptide transport carrier in the human intestinal cell line, Caco-2. Biochim Biophys Acta 1990;1027:211–7.
[20] Saito S, Murakami Y, Miyauchi S, Kamo N. Measurement of plasma membrane potential in isolated rat hepatocytes using the lipophilic cation, tetraphenylphosphonium: correction of probe intracellular binding and mitochondrial accumulation. Biochim Biophys Acta 1992;1111:221–30.
[21] Zanker V, Peter W. Die prototropen formen des fluoresceins. Chem Ber 1958;91:572–80.
[22] Lindquist L. A flash photolysis study of fluorescein. Ark Kemi 1960; 16:79–138.
[23] Sjoback R, Nygren J, Kubista M. Absorption and fluorescence properties of fluorescein. Spectrochim Acta A Mol Biomol Spectrosc 1995;51:L7–21.
[24] Prichard JB, Miller DS. Mechanisms mediating renal secretion of organic anions and cations. Physiol Rev 1993;73:765–96.
[25] Sweet DH, Wolff NA, Prichard JB. Expression cloning and characterization of ROAT1. J Biol Chem 1997;272:30088–95.
[26] Wong MH, Oelkers P, Craddock AL, Dawson PA. Expression cloning and characterization of the hamster ileal sodium-dependent bile acid transporter. J Biol Chem 1994;269:1340–7.
[27] Simanjuntak MT, Tamai I, Terasaki T, Tsuji A. Carrier-mediated uptake of nicotinic acid by rat intestinal brush-border membrane vesicles and relation to monocarboxylic acid transport. J Pharmacobiodyn 1990;13:301–9.
[28] Takanaga H, Tamai I, Terasaki T, Tsuji A. pH-dependent, and carrier-mediated transport of salicylic acid across Caco-2 cells. J Pharm Pharmacol 1994;46:567–70.
[29] Tsuji A, Takanaga H, Tamai I, Terasaki T. Transcellular transport of benzoic acid across Caco-2 cells by a pH-dependent and carrier-mediated transport mechanism. Pharm Res 1994;11:30–7.
[30] Tamai I, Takanaga H, Maeda H, Ogihara T, Yoneda M, Tsuji A. Proton-cotransport of pravastatin across intestinal brush-border membrane. Pharm Res 1996;12:1727–32.
[31] Takagi M, Taki Y, Sakane T, Nadai T, Sezaki H, Oku N, Yamashita S. A new interpretation of salicylic acid transport across the lipid bilayer: implications of pH-dependent but not carrier-mediated absorption from the gastrointestinal tract. J Pharmacol Exp Ther 1998; 285:1175–80.
[32] Price NT, Jackson VN, Halestrap AP. Cloning and sequencing of four new mammalian monocarboxylate transporter (MCT) homologues confirms the existence of a transporter family with an ancient past. Biochem J 1998;329:321–9.
[33] Halestrap AP, Price NT. The proton-linked monocarboxylate transporter (MCT) family: structure, function and regulation. Biochem J 1999;343:281–99.
[34] Broer S, Rahman B, Pellegri G, Pellerin L, Martin J-L, Verleysdonk S, Hamprecht B, Magistretti PJ. Comparison of lactate transport in astroglial cells and monocarboxylate transporter 1 (MCT 1) expressing *Xenopus laevis* oocytes. J Biol Chem 1997;272:30096–102.
[35] Garcia CK, Brown MS, Pathak RK, Goldstein JL. cDNA cloning of MCT2, a second monocarboxylate transporter expressed in different cells than MCT1. J Biol Chem 1995;270:1843–9.
[36] Wilson MC, Jackson VN, Heddle C, Price NT, Pilegaard H, Juel C, Bonen A, Montgomery I, Hutter OF, Halestrap AP. Lactic acid efflux from white skeletal muscle is catalyzed by the monocarboxylate transporter isoform MCT3. J Biol Chem 1998;273:15920–6.
[37] Juel C, Halestrap AP. Lactate transport in skeletal muscle—role and regulation of the monocarboxylate transporter. J Physiol (Lond) 1999; 517:633–42.
[38] Broer S, Schneider HP, Broer A, Rahman B, Hamprecht B, Deitmer JW. Characterization of the monocarboxylate transporter 1 expressed in *Xenopus laevis* oocytes by changes in cytosolic pH. Biochem J 1998;333:167–74.
[39] Lin R-Y, Vera JC, Chaganti RSK, Golde DW. Human monocarboxylate transporter 2 (MCT2) is a high affinity pyruvate transporter. J Biol Chem 1988;273:28959–65.
[40] Ritzhaupt A, Wood IS, Ellis A, Hosie KB, Shirazi-Beechey SP. Identification and characterization of a monocarboxylate transporter (MCT1) in pig and human colon: its potential to transport l-lactate as well as butyrate. J Physiol (Lond) 1998;513:719–32.
[41] Lamers JMJ. Some characteristics of monocarboxylic acid transfer across the cell membrane of epithelial cells from rat small intestine. Biochim Biophys Acta 1975;413:265–76.